Yukawa corrections to the bottom pair production in photon-photon collisions

Han Liang,[2] Cheng-Guo Hu,[3] Chong-Sheng Li,[1,4] and Ma Wen-Gan[1,2]
[1]*China Center of Advanced Science and Technology (World Laboratory), P.O. Box 8730, Beijing 100080, People's Republic of China*
[2]*Department of Modern Physics, University of Science and Technology of China (USTC), Hefei, Anhui 230027, People's Republic of China**
[3]*Department of Physics, Chongqing University, Chongqing, Sichuan 630044, People's Republic of China*
[4]*Physics Department, Peking University, Beijing 100871, People's Republic of China*

(Received 26 September 1995; revised manuscript received 20 February 1996)

The $O(\alpha m_t^2/m_W^2)$ Yukawa corrections to bottom quark pair production via photon-photon fusion in TeV e^+e^- colliders are calculated in both the general two-Higgs-doublet model and minimal supersymmetric model. We find that the corrections to the cross section of the subprocess $\gamma\gamma\rightarrow b\bar{b}$ can be a few percent. The corrections to the total cross section of the process $e^+e^-\rightarrow\gamma\gamma\rightarrow b\bar{b}$ in the beamstrahlung photon fusion mode are rather small and can be ignored at the one-loop level; however, the corrections in the Compton backscattering photon fusion mode may approach 0.1% for favorable parameter values. [S0556-2821(96)04315-9]

PACS number(s): 14.65.Fy, 12.38.Bx, 13.60.−r

I. INTRODUCTION

The collisions of high energy photons produced at the next-generation linear collider (NLC) provide a comprehensive laboratory for testing the standard model (SM) and probing new physics beyond the SM [1]. There are mainly two options for the photon sources at the NLC: laser backscattering and beamstrahlung photons. These two kinds of photon sources are the options of turning the electron-positron collider into a laser photon collider with high energy and high luminosity. With the advent of the new collider technique [2], one can obtain the high energy and high intensity photon beams by using Compton laser photons scattering off the colliding electron and positron beams. The luminosity and energy of colliding photons are expected to be comparable to that of the primary e^+e^- collisions. This mechanism is the so-called laser backscattering photon collision mode, which can be employed in the NLC. The beamstrahlung is another way in obtaining photons. The strong electromagnetic fields associated with the high charge density in such bunches subject particles to very strong accelerating forces just prior to or during the collision. As a result the so-called beamstrahlung photons [3] are radiated. It has been shown that the first photon source may have a more interesting physical potential. Actually with any of the photon sources there are no known overwhelming obstacles in building such a machine. By means of such a collider a large number of heavy quark pairs can be produced by beamstrahlung and Compton backscattering which will reach a center-of-mass energy of 500–2000 GeV with a luminosity of the order of 10^{33} cm^{-2} s^{-1}. The photon energy spectrums in both modes [4,5] show that there are many relatively soft photons especially in beamstrahlung mode and the production of heavy top quark will be suppressed for reduced collision energies. But no such suppression affects the relatively light bottom quark. For instance, in beamstrahlung photon collision the bottom-quark pair are predominantly produced at all energies with yields exceeding those calculated from the annihilation process by a factor 10^3 at 1 TeV [6]. We know that since $H^0\rightarrow b\bar{b}$ would be the main search channel for a standard H^0 [or lightest minimal supersymmetric standard model (MSSM) h^0] with mass less than about 130 GeV, the precise study of the main background process $\gamma\gamma\rightarrow b\bar{b}$ is very necessary. In the SM this process have been calculated and the QCD threshold effects of the process also have been examined [7]. However, in a two-Higgs-doublet model (2HDM), the production of the bottom quark receives an additional correction arising from the Yukawa coupling of the bottom to the top quark. Once the top quark mass is known precisely, this effect could be used as an indirect test between the SM and other models which include the 2HDM and the MSSM.

Therefore it is worthy to investigate the production of the bottom quark pairs in $\gamma\gamma$ collisions produced by photon-photon colliders. In this work, we present the calculation of the $O(\alpha m_t^2/m_W^2)$ Yukawa corrections in both 2HDM and MSSM, which arise from the virtual effects of third family (top and bottom) quarks, charged Higgs and charged Goldston bosons ($G^{\pm}$) in photon-photon collisions via both beamstrahlung and Compton back-scattering modes. In Sec. II, we present the analytical results in terms of the well-known standard notations of one-loop Feynman integrals [8]. In Sec. III, we present some numerical examples and discuss the implication of our results, which involve the correction results in both photon collision modes. And in the Appendix we list explicitly the form factors appeared in the cross section.

II. CALCULATIONS

The relevant Feynman diagrams are shown in Fig. 1 and the Feynman rules can be found in [9]. In our calculation, we use dimensional regularization to regulate all the ultraviolet divergences in the virtual loop corrections and we adopt the on-mass-shell renormalization scheme [10,11]. Taking into account the $O(\alpha m_t^2/m_W^2)$ Yukawa corrections, the renormalized amplitude for $\gamma\gamma\rightarrow b\bar{b}$ is given by

*Mailing address.

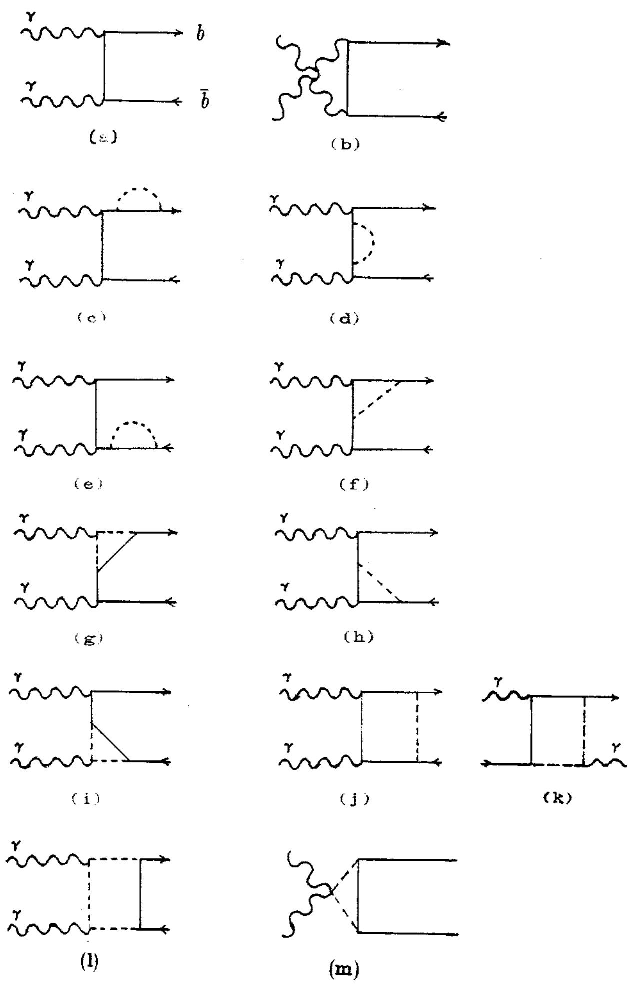

FIG. 1. Feynman diagrams contributing to $O(\alpha m_t^2/m_W^2)$ Yukawa corrections to $\gamma\gamma\to b\bar{b}$: (a),(b) tree-level diagrams; (c)–(e) self-energy diagrams; (f)–(i) vertex diagrams; (j)–(l) box diagrams; (m) triangle diagrams. Here we only plot the one-loop diagrams corresponding to the tree-level diagram (a). The dashed lines represent $H^\pm$, $G^\pm$ for (c)–(m).

$$M_{\rm ren}=M_0+\delta M_{1\ \rm loop}=M_0+\delta M^{\rm self}+\delta M^{\rm vertex}+\delta M^{\rm box}+\delta M^{\rm tr}, \tag{1}$$

where M_0 is the amplitude at the tree level, $\delta M^{\rm self}$, $\delta M^{\rm vertex}$, $\delta M^{\rm box}$, and $\delta M^{\rm tr}$ represent the $O(\alpha m_t^2/m_W^2)$ Yukawa corrections arising from the self-energy, vertex, box, and triangle diagrams, respectively. Their explicit forms are given by

$$M_0=M_0^{\hat t}+M_0^{\hat u}, \tag{2}$$

$$\delta M^{\rm self}=\delta M^{s(\hat t)}+\delta M^{s(\hat u)}, \tag{3}$$

$$\delta M^{\rm vertex}=\delta M^{v(\hat t)}+\delta M^{v(\hat u)}, \tag{4}$$

$$\delta M^{\rm box}=\delta M^{b(\hat t)}+\delta M^{b(\hat u)}, \tag{5}$$

where

$$M_0^{\hat t}=-i\,\frac{e^2Q_b^2}{\hat t-m_b^2}\,\epsilon_\mu(p_4)\epsilon_\nu(p_3)\overline{u(p_2)}\times\gamma^\mu(\not p_2-\not p_4+m_b)\gamma^\nu v(p_1), \tag{6}$$

$$M_0^{\hat u}=M_0^{\hat t}(p_3\leftrightarrow p_4,\hat t\to\hat u), \tag{7}$$

$$\delta M^{s(\hat t)}=i\,\frac{e^2Q_b^2}{(\hat t-m_b^2)^2}\,\epsilon_\mu(p_4)\epsilon_\nu(p_3)\overline{u(p_2)}(f_1^{s(\hat t)}\gamma^\mu\gamma^\nu+f_2^{s(\hat t)}p_2^\mu\gamma^\nu+f_3^{s(\hat t)}\not p_4\gamma^\mu\gamma^\nu)v(p_1), \tag{8}$$

$$\delta M^{s(\hat u)}=\delta M^{s(\hat t)}(p_3\leftrightarrow p_4,\hat t\to\hat u), \tag{9}$$

$$\delta M^{v(\hat t)}=-i\,\frac{e^2Q_b}{\hat t-m_b^2}\,\epsilon_\mu(p_4)\epsilon_\nu(p_3)\overline{u(p_2)}(f_1^{v(\hat t)}\gamma^\mu\gamma^\nu+f_2^{v(\hat t)}p_1^\nu\gamma^\mu+f_3^{v(\hat t)}p_2^\mu\gamma^\nu+f_4^{v(\hat t)}p_2^\mu p_1^\nu+f_5^{v(\hat t)}\not p_4\gamma^\mu\gamma^\nu+f_6^{v(\hat t)}\not p_4p_1^\nu\gamma^\mu+f_7^{v(\hat t)}\not p_4p_2^\mu\gamma^\nu)v(p_1), \tag{10}$$

$$\delta M^{v(\hat u)}=\delta M^{v(\hat t)}(p_3\leftrightarrow p_4,\hat t\to\hat u), \tag{11}$$

$$\begin{aligned}\delta M^{b(\hat t)}=-i\,\frac{e^2}{16\pi^2}\,\epsilon_\mu(p_4)\epsilon_\nu(p_3)\overline{u(p_2)}[&f_1^{b(\hat t)}\gamma^\mu\gamma^\nu+f_2^{b(\hat t)}\gamma^\nu\gamma^\mu+f_3^{b(\hat t)}p_1^\nu\gamma^\mu+f_4^{b(\hat t)}p_1^\mu\gamma^\nu+f_5^{b(\hat t)}p_2^\nu\gamma^\mu\\&+f_6^{b(\hat t)}p_2^\mu\gamma^\nu+f_7^{b(\hat t)}p_1^\mu p_1^\nu+f_8^{b(\hat t)}p_1^\mu p_2^\nu+f_9^{b(\hat t)}p_2^\mu p_1^\nu\\&+f_{10}^{b(\hat t)}p_2^\mu p_2^\nu+f_{11}^{b(\hat t)}\not p_4\gamma^\mu\gamma^\nu+f_{12}^{b(\hat t)}\not p_4\gamma^\nu\gamma^\mu\\&+f_{13}^{b(\hat t)}\not p_4p_1^\nu\gamma^\mu+f_{14}^{b(\hat t)}\not p_4p_1^\mu\gamma^\nu+f_{15}^{b(\hat t)}\not p_4p_2^\nu\gamma^\mu\\&+f_{16}^{b(\hat t)}\not p_4p_2^\mu\gamma^\nu+f_{17}^{b(\hat t)}\not p_4p_1^\mu p_1^\nu+f_{18}^{b(\hat t)}\not p_4p_1^\mu p_2^\nu\\&+f_{19}^{b(\hat t)}\not p_4p_2^\mu p_1^\nu+f_{20}^{b(\hat t)}\not p_4p_2^\mu p_2^\nu]v(p_1),\end{aligned} \tag{12}$$

$$\delta M^{b(\hat u)}=\delta M^{b(\hat t)}(p_3\leftrightarrow p_4,\hat t\leftrightarrow\hat u), \tag{13}$$

$$\delta M^{\rm tr}=i\,\frac{e^2}{16\pi^2}\,f_1^{\rm tr}2g^{\mu\nu}\epsilon^\mu(p_4)\epsilon^\nu(p_3)\overline{u(p_2)}v(p_1). \tag{14}$$

Here $\hat t=(p_4-p_2)^2$, $\hat u=(p_1-p_4)^2$, p_3, and p_4 denote the momentum of the two incoming photons, and p_2 and p_1 are momentum of the outgoing bottom quark and its antiparticle. The form factors $f_i^{s(\hat t)},f_i^{v(\hat t)},f_i^{b(\hat t)},f_i^{\rm tr}$ are presented in Appendix A.

The cross section of the subprocess for the unpolarized photons is given by

$$\hat\sigma(\hat s)=\frac{N_C}{16\pi\hat s^2}\int_{\hat t^-}^{\hat t^+}d\hat t\overline{\sum_{\rm spins}}|M_{\rm ren}(\hat s,\hat t)|^2, \tag{15a}$$

where $\hat t^\pm=(m_b^2-\frac{1}{2}\hat s)\pm\frac{1}{2}\hat s\beta_b$, $\beta_b=\sqrt{1-4m_b^2/\hat s}$, and N_C in the above equation is the number of colors. The bar over the sum recalls averaging over initial spins and

$$\overline{\sum_{\text{spins}}} |M_{\text{ren}}(\hat{s},\hat{t})|^2 = \overline{\sum_{\text{spins}}} |M_0|^2 + 2\,\text{Re}\left(\overline{\sum_{\text{spins}}} M_0^\dagger \delta M_{1\ \text{loop}}\right). \tag{15b}$$

The differential cross section at the tree level, which is contributed from the first term in the above equation, is given by [6]

$$\frac{\partial\hat{\sigma}_0}{\partial\hat{t}} = \frac{6\pi\alpha^2 Q_b^4}{\hat{s}^2}\left(\frac{m_b^2-\hat{u}}{m_b^2-\hat{t}} + \frac{m_b^2-\hat{t}}{m_b^2-\hat{u}} + \frac{2m_b^2(\hat{s}-4m_b^2)}{(m_b^2-\hat{t})(m_b^2-\hat{u})} - \frac{2m_b^2(m_b^2+\hat{t})}{(m_b^2-\hat{t})^2} - \frac{2m_b^2(m_b^2+\hat{u})}{(m_b^2-\hat{u})^2}\right). \tag{15c}$$

The explicit expression of the interference term in Eq. (15b) can be found in Appendix B. The total cross section for bottom quark pair production can be obtained by folding the cross section $\hat{\sigma}$ for the subprocesses with the photon luminosity

$$\sigma(s) = \int_{2m_b/\sqrt{s}}^{x_{\max}} dz\, \frac{dL_{\gamma\gamma}}{dz}\, \hat{\sigma}(\gamma\gamma - b\bar{b} \ \text{at} \quad \hat{s}=z^2 s), \tag{16}$$

where $\sqrt{s}$ and $\sqrt{\hat{s}}$ are the e^+e^- and $\gamma\gamma$ center-of-mass energies, respectively, and the quantity $dL_{\gamma\gamma}/dz$ is the photon luminosity, which can be expressed as

$$\frac{dL_{\gamma\gamma}}{dz} = 2z\int_{x^2/x_{\max}}^{x_{\max}} \frac{dx}{x}\, f_{\gamma/e}(x) f_{\gamma/e}(z^2/x), \tag{17}$$

where $f_{\gamma/e}$ is the photon structure function of the electron beam [6,4,12]. For a TeV collider with elliptic beams with $\sigma_x/\sigma_y=25.5$, the beamstrahlung photon structure function can be represented as [4]

$$f_{\gamma/e}^{\text{beam}} = \begin{cases} \left(2.25 - \sqrt{\dfrac{x}{0.166}}\right)\left(\dfrac{1-x}{x}\right)^{2/3} & \text{for } x<0.84, \\ 0 & \text{for } x>0.84, \end{cases} \tag{18}$$

where x is the relative momentum of the radiated photon and the parent electron.

If we operate NLC as a mother machine of photon-photon collider in Compton backscattering photon fusion mode, the energy spectrum of the photons is given by [5]

$$f_{\gamma/e}^{\text{Comp}} = \begin{cases} \dfrac{1}{1.8397}\left(1-x+\dfrac{1}{1-x} - \dfrac{4x}{x_i(1-x)} + \dfrac{4x^2}{x_i^2(1-x)^2}\right) & \text{for } x<0.83,\ x_i=2(1+\sqrt{2}), \\ 0 & \text{for } x>0.83. \end{cases} \tag{19}$$

III. NUMERICAL EXAMPLES AND CONCLUSION

In the numerical evaluation we take a set of independent input parameters which are known from current experiments. The input parameters [13] are $m_b=4.5$ GeV, $m_Z=91.1887$ GeV, $m_W=80.2226$ GeV, and $G_F=1.166\,392\times10^{-5}$ $(\text{GeV})^{-2}$; $\alpha=1/137.036$. The top quark mass is just fixed to be the central value $m_t=175$ GeV. It is known that the cross section for the $e^+e^-\to\gamma\gamma\to b\bar{b}$ at the tree level, is model independent, which has already calculated in Ref. [6], but the quantum corrections are model dependent. The correction quantity is related to the additional parameters in 2HDM and MSSM.

The parameter $\tan\beta$ is chosen to be varied in our calculation. As we know, the coupling strength of the charged Higgs bosons with quarks is related to scalar and pseudoscalar parts, which have factors A_{H^+} and B_{H^+}, respectively. (The definitions of A_{H^+} and B_{H^+} can be found in Appendix A.) These two parts of Yukawa coupling yield the crucial correction alternatively depending on variate $\tan\beta$. The coupling strength relies mostly on the factor with top quark mass if $\tan\beta\ll1$, while the bottom mass part might take the major role in case $\tan\beta\gg1$. Because of the present experiments, the small values of $\tan\beta$ are in disfavor both in 2HDM and in MSSM. In the numerical calculation, we limit its value to be in the range of 1 to 70. The correction result of calculation is depicted in Fig. 2, on conditions of $m_{H^\pm}=150$ GeV and $\sqrt{\hat{s}}=500$ GeV. From the graph we can see that when $\tan\beta$ is slightly bigger than 1, the coupling strength from the term with bottom mass cannot overwhelm that from the term with top mass. This status will keep unchanged until $\tan\beta>10$. The relative correction δ, which is defined as $\hat{\sigma}-\hat{\sigma}_0/\hat{\sigma}_0$, is only about 0.5% at the point $\tan\beta=10$. Although the correction will be increased with the increment of $\tan\beta$, it is not directly proportional to $\tan^2\beta$.

In the MSSM, the neutral Higgs sector masses and α can be computed by the input parameters m_Z, m_W, $m_{H^\pm}$, and

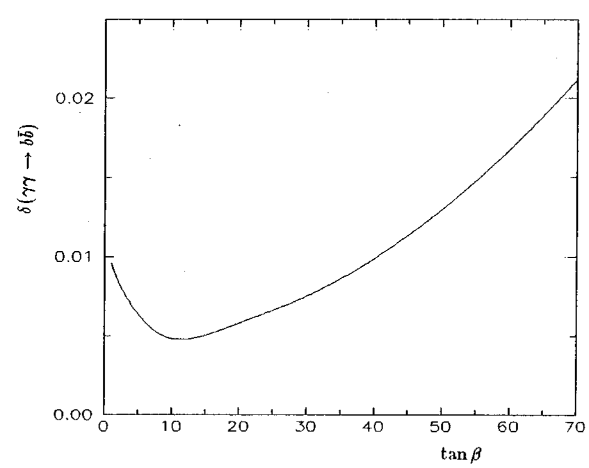

FIG. 2. The relative correction of the subprocess $\gamma\gamma\to b\bar{b}$ as a function of $\tan\beta$, when $\sqrt{\hat{s}}=500$ GeV and $m_{H^\pm}=150$ GeV.

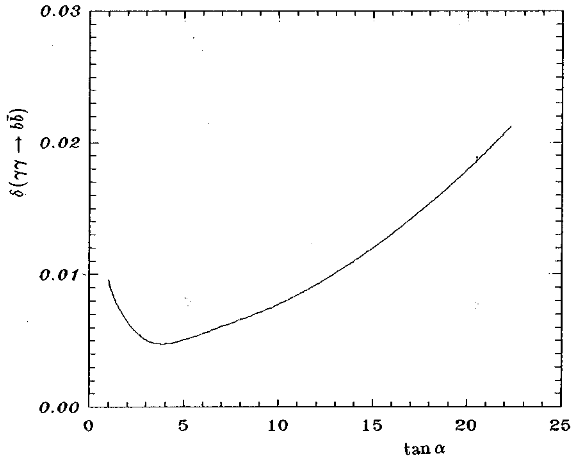

FIG. 3. The relative correction of the subprocess $\gamma\gamma \to b\bar{b}$ as a function of tan α, when $\sqrt{\hat{s}}$=500 GeV and $m_{H^\pm}$=150 GeV.

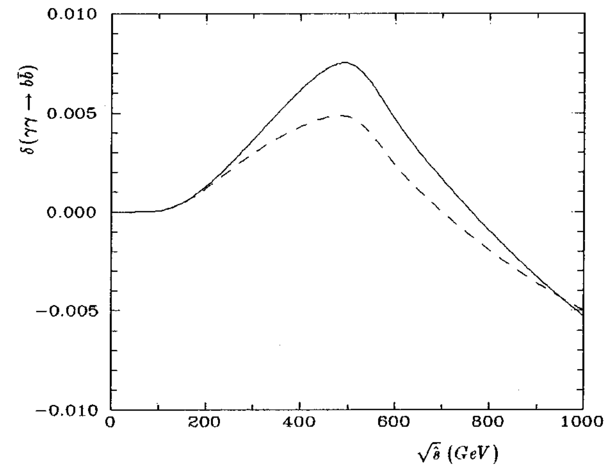

FIG. 5. The relative correction of the subprocess $\gamma\gamma \to b\bar{b}$ as a function of $\sqrt{\hat{s}}$, when $m_{H^\pm}$=150 GeV. The dashed line and solid line are for tan β=10 and 30, respectively.

tan β. The formulas are given as

$$m_A^2 = m_{H^\pm}^2 - m_W^2,$$

$$\tan 2\alpha = \frac{m_A^2 + m_Z^2}{m_A - m_Z^2} \tan 2\beta. \qquad (20)$$

In Fig. 3 the relation between the relative correction with the parameter tan α in MSSM is plotted, in which we limit α to be in the range of 0°∼90°. The curve is very similar to Fig. 2.

Since the present experimental results give constraint on the charged Higgs boson mass only as $m_{H^\pm} \geqslant \frac{1}{2} m_Z$, we investigate the effect coming from charged Higgs boson mass in the range 50 to 600 GeV. The curve in Fig. 4 shows its correction results with $\sqrt{\hat{s}}$=500 GeV. From that figure we can see, though there is a small mound when $m_{H^\pm}<250$ GeV, the curve is going to be flat when $m_{H^\pm}>300$ GeV, and the difference between the top of the mound and the bottom of the line is less than 7%. All of these imply that variance of the Yukawa corrections coming from the different Higgs boson mass values is rather small.

In Fig. 5 the relative Yukawa corrections for the cross section of bottom pair production in photon-photon collision, are illustrated as functions of the center-of-mass $\sqrt{\hat{s}}$ with $m_{H^\pm}$=150 GeV. The solide curve is for tan β=30, and the dashed one for tan β=10, respectively. Both of the curves are rather flat in the low energy area ($\sqrt{\hat{s}}<100$ GeV), and the relative corrections approach to be zero. That is owing to the large contribution of tree level $\hat{\sigma}_0$. The figure shows also each curve has a peak about $\sqrt{\hat{s}}$=500 GeV for the different values of tan β.

In studying the beamstrahlung photon collision for the bottom quark pair production, we find that the contribution from the low energy range of the subprocess cross section, will dominate over that from the high energy range during consolution with the beamstrahlung luminosity Eq. (18). That is to say the beamstrahlung photons are relatively soft and the Yukawa corrections rely mostly on the low energy

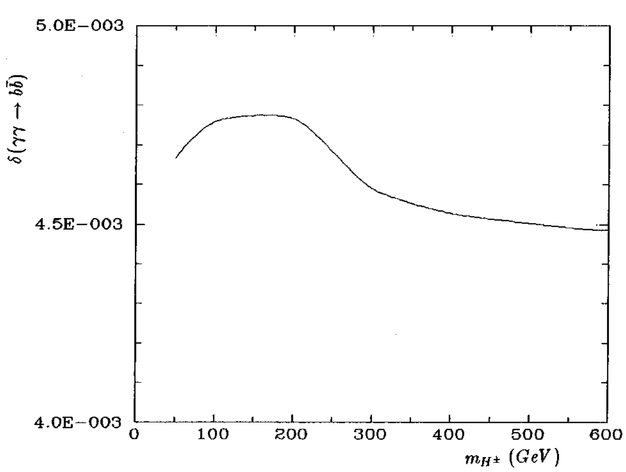

FIG. 4. The relative correction of the subprocess $\gamma\gamma \to b\bar{b}$ as a function of $m_{H^\pm}$, when $\sqrt{\hat{s}}$=500 GeV and tan β=10.

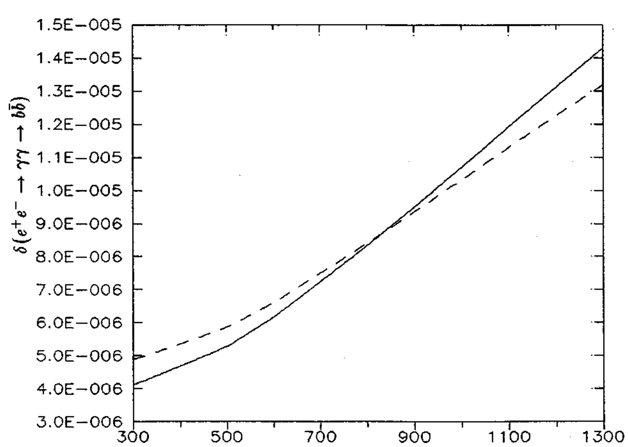

FIG. 6. The relative correction of the process $e^+e^- \to \gamma\gamma \to b\bar{b}$ in beamstrahlung photon mode as a function of $\sqrt{s}$, when $m_{H^\pm}$ =150 GeV. The dashed line and solid line are for tan β=10 and 30, respectively.

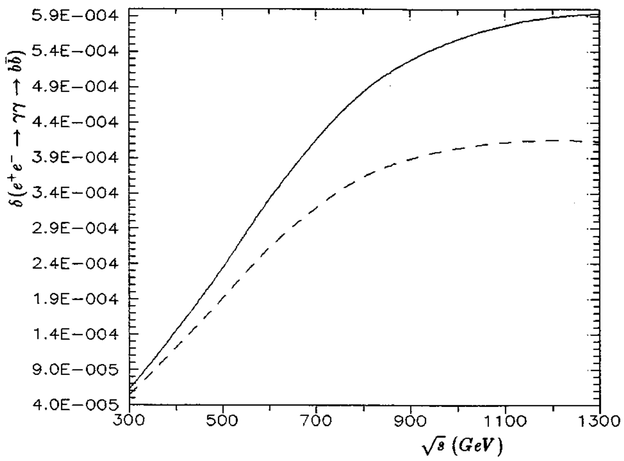

FIG. 7. The relative correction of the process $e^+e^-\to\gamma\gamma\to b\overline{b}$ in backscattering laser mode as a function of $\sqrt{s}$, when $m_{H^\pm}=150$ GeV. The dashed line and solid line are for tan β=10 and 30, respectively.

beamstrahlung photon. That will suppress the relative correction for the process $e^+e^-\to\gamma\gamma\to b\bar{b}$ in beamstrahlung photon mode rather heavily. All these can be seen in Fig. 6, where the Yukawa corrections to the total cross section for bottom pair production in beamstrahlung photon mode during e^+e^- collision, are plotted as the functions of center-of-mass $\sqrt{s}$ with tan β=10 and 30, respectively. The contribution is only about 10^{-6}–10^{-5}. However, by using backscattering laser collision, the relative correction shows large enhancement compared to that by using beamstrahlung photon collision. In Fig. 7 we plot out the relative corrections of the total cross section of the same process in backscattering laser collision mode, also as functions of $\sqrt{s}$. From the graph, the largest correction can reach the value of 6×10^{-4}, nearly two order higher than the corresponding correction in beamstrahlung photon collision mode. This correction can be expected to reach the order of 10^{-3} with the tan β larger than 30 or the center of mass of the laser collision higher than 1.3 TeV.

In conclusion, we have calculated the $O(\alpha m_t^2/m_W^2)$ Yukawa corrections to the process of $\gamma\gamma\to b\bar{b}$. The corrections are model dependent. For the favorable parameters, the corrections give out a 1–3% increment of the cross section from tree level, when tan β is in the range of 1 to 70, $\sqrt{s}$=500 GeV and $m_{H^\pm}=150$ GeV. The total cross section of the process $e^+e^-\to\gamma\gamma\to b\bar{b}$ are also calculated for both beamstrahlung and backscattering laser beam collisions with the same mother e^+e^- collider. To the beamstrahlung photon source, because of the large contribution of the low photon energy range, the correction to the total cross section at the tree level is very small, and we can ignore it in one-loop level. However, the backscattering laser collision mode is much promising, which implies near 0.1% correction to the tree level.

ACKNOWLEDGMENTS

This work was supported in part by the National Natural Science Foundation of China and the National Committee of Science and Technology of China.

APPENDIX A

The form factors $f_i^{s(\hat{t})}$ can be expressed by

$$f_1^{s(\hat{t})}=-2m_b(p_2\cdot p_4)\left[\Sigma_S^b(\hat{t})-\frac{\delta m_b}{m_b}-\delta Z_V^b\right]$$
$$-2m_b(p_2\cdot p_4)[\Sigma_V^b(\hat{t})+\delta Z_V^b],$$

$$f_2^{s(\hat{t})}=4m_b^2\left[\Sigma_S^b(\hat{t})-\frac{\delta m_b}{m_b}-\delta Z_V^b\right]$$
$$+4(m_b^2-p_2\cdot p_4)[\Sigma_V^b(\hat{t})+\delta Z_V^b],$$

$$f_3^{s(\hat{t})}=\frac{1}{2}f_2^{s(\hat{t})},$$

where Σ^b, δm_b, and δZ_V^b are Yukawa contribution part of the unrenormalized self-energy function, b-quark mass, and wave function renormalization constants, respectively. Their expressions are listed as

$$\Sigma^b(p^2)=\not{p}[\Sigma_V^b(p^2)+\gamma_5\Sigma_A^b(p^2)]+m_b\Sigma_S^b(p^2).$$

Actually the Σ_A^b does not contribute to the form factor f_i^s, since the term with Σ_A^b includes γ_5:

$$\Sigma_V^b(p^2)=\frac{-\alpha}{8\pi m_W^2 s_W^2}\sum_{i=H^+,G^+}(m_t^2\eta_i$$
$$+m_b^2\eta_i^{-1})B_1(p^2,m_t,m_i),$$

$$\Sigma_A^b(p^2)=\frac{\alpha}{8\pi m_W^2 s_W^2}\sum_{i=H^+,G^+}(m_t^2\eta_i$$
$$-m_b^2\eta_i^{-1})B_1(p^2,m_t,m_i),$$

$$\Sigma_S^b(p^2)=\frac{\alpha m_t^2}{8\pi m_W^2 s_W^2}[B_0(p^2,m_t,m_{H^\pm})-B_0(p^2,m_t,m_W)],$$

$$\delta m_b=m_b^2[\Sigma_V^b(m_b^2)+\Sigma_S^b(m_b^2)],$$

$$\delta Z_V^b=-\Sigma_V^b(m_b^2)-2m_b^2[\Sigma_V^{b'}(m_b^2)+\Sigma_S^{b'}(m_b^2)],$$

where we denote

$$\Sigma_{V,S}^{b'}(m_b^3)=\frac{\partial\Sigma_{V,S}^b(k^2)}{\partial k^2}\Bigg|_{k^2=m_b^2}.$$

We define $g_i^+=(A_i^2+B_i^2)$ and $g_i^-=(A_i^2-B_i^2)$ $(i=H^+$ and $G^+)$ where

$$A_{H^+}=\frac{ig}{2\sqrt{2}m_W}(m_t\cot\beta+m_b\tan\beta),$$

$$B_{H^+}=\frac{ig}{2\sqrt{2}m_W}(m_b\tan\beta-m_t\cot\beta),$$

$$A_{G^+}=\frac{-ig}{2\sqrt{2}m_W}(m_b-m_t),$$

$$B_{G^+}=\frac{-ig}{2\sqrt{2}m_W}(m_b+m_t).$$

We denote $d=4-\epsilon$ in the following expressions. The form factors $f_i^{v(\hat{t})}$, $f_i^{b(\hat{t})}$, and $f_i^{\rm tr}$ are given by

$$f_1^{v(\hat{t})}=\frac{Q_t}{8\pi^2}(p_2\cdot p_4)\sum_{i=H^+,G^+}[g_i^+m_b\{(C_0+C_{11})[p_2,-p_4,m_i,m_t,m_t]+(C_0+C_{11})[-p_1,p_3,m_i,m_t,m_t]\}$$
$$+g_i^-m_t\{C_0[p_2,-p_4,m_i,m_t,m_t]+C_0[-p_1,p_3,m_i,m_t,m_t]\}],$$

$$f_2^{v(\hat{t})}=\frac{-1}{4\pi^2}(p_2\cdot p_4)\sum_{i=H^+,G^+}g_i^+\{Q_t(C_{12}+C_{23})[-p_1,p_3,m_i,m_t,m_t]+(C_{12}+C_{23})[p_1,-p_3,m_t,m_i,m_i]\},$$

$$f_3^{v(\hat{t})}=\frac{1}{8\pi^2}\sum_{i=H^+,G^+}[g_i^+\{Q_t((2-d)C_{24}-m_b^2(C_0+2C_{11}+C_{21})-m_t^2C_0)[p_2,-p_4,m_i,m_t,m_t]+2(C_{24}-m_b^2(C_{11}+C_{21})$$
$$+(p_2\cdot p_4)(C_{12}+C_{23}))[-p_2,p_4,m_t,m_i,m_i]+Q_t((2-d)C_{24}-m_b^2(C_0-C_{21}-2C_{22}+2C_{23})-m_t^2C_0$$
$$+2(p_1\cdot p_2-p_1\cdot p_4)(C_{22}-C_{23})-2(p_2\cdot p_4)(C_{12}+C_{22}))[-p_1,p_3,m_i,m_t,m_t]+2C_{24}[p_1,-p_3,m_t,m_i,m_i]\}$$
$$+g_i^-2m_bm_t\{(C_0+C_{11})[-p_2,p_4,m_t,m_i,m_i]-Q_t(C_0+C_{11})[p_2,-p_4,m_i,m_t,m_t]-Q_tC_0[-p_1,p_3,m_i,m_t,m_t]\}]$$
$$+4Q_b\delta Z_V^b,$$

$$f_4^{v(\hat{t})}=\frac{1}{4\pi^2}\sum_{i=H^+,G^+}[g_i^+m_b\{Q_t(C_{11}+C_{21})[-p_1,p_3,m_i,m_t,m_t]+(C_{11}+C_{21})[p_1,-p_3,m_t,m_i,m_i]\}$$
$$+g_i^-m_t\{Q_tC_{11}[-p_1,p_3,m_i,m_t,m_t]-(C_0+C_{11})[p_1,-p_3,m_t,m_i,m_i]\}],$$

$$f_5^{v(\hat{t})}=\frac{1}{16\pi^2}\sum_{i=H^+,G^+}[g_i^+\{Q_t((2-d)C_{24}-m_b^2(C_0-C_{21})-m_t^2C_0-2(p_2\cdot p_4)(C_{12}+C_{23}))[p_2,-p_4,m_i,m_t,m_t]$$
$$+Q_t((2-d)C_{24}-m_b^2(C_0-C_{21}-2C_{22}+2C_{23})-m_t^2C_0+2(p_1\cdot p_2-p_1\cdot p_4)(C_{22}-C_{23})$$
$$-2(p_2\cdot p_4)(C_{12}+C_{22}))[-p_1,p_3,m_i,m_t,m_t]+2C_{24}[-p_2,p_4,m_t,m_i,m_i]+2C_{24}[p_1,-p_3,m_t,m_i,m_i]\}$$
$$-2g_i^-m_bm_tQ_t\{C_0[p_2,-p_4,m_i,m_t,m_t]+C_0[-p_1,p_3,m_i,m_t,m_t]\}]+2Q_b\delta Z_V^b,$$

$$f_6^{v(\hat{t})}=\frac{1}{2}f_4^{v(\hat{t})},$$

$$f_7^{v(\hat{t})}=\frac{1}{8\pi^2}\sum_{i=H^+,G^+}[g_i^+m_b\{Q_t(C_{11}+C_{21})[p_2,-p_4,m_i,m_t,m_t]+(C_{11}+C_{21})[-p_2,p_4,m_t,m_i,m_i]\}$$
$$+g_i^-m_t\{Q_tC_{11}[p_2,-p_4,m_i,m_t,m_t]-(C_0+C_{11})[-p_2,p_4,m_t,m_i,m_i]\}],$$

$$f_1^{b(\hat{t})}=\sum_{i=H^+,G^+}[g_i^+\{Q_t^2(4m_b(D_{27}+D_{311})-m_b^3(D_0+3D_{11}-2D_{13}+3D_{21}+2D_{23}-4D_{25}+D_{31}-2D_{35}+2D_{37})+m_bm_t^2(D_0+D_{11})+m_b2(p_1\cdot p_2)(D_{13}-D_{23}+2D_{25}+D_{35}-D_{37})-2m_b(p_1\cdot p_4)(D_{13}-D_{23}+D_{25}+D_{26}+D_{310}-D_{37})+2m_b(p_2\cdot p_4)(D_{11}+D_{12}-2D_{13}+D_{21}+D_{23}+2D_{24}-3D_{25}-D_{26}-D_{310}+D_{34}-D_{35}+D_{37}))\times[p_2,-p_4,-p_3,m_i,m_t,m_t,m_t]+2m_bD_{311}[-p_2,p_4,p_3,m_t,m_i,m_i,m_i]+2m_bQ_t(D_{312}-D_{27}-D_{311}-D_{313})\times[-p_1+p_3,p_1,-p_1+p_4,m_i,m_t,m_i,m_t]\}+g_i^-m_t\{Q_t^2(2D_{27}-m_b^2(D_0+2D_{11}-2D_{13}+D_{21}+2D_{23}-2D_{25})+m_t^2D_0+2(p_1\cdot p_2)(D_{13}-D_{23}+D_{25})-2(p_1\cdot p_4)(D_{13}-D_{23}+D_{26})+2(p_2\cdot p_4)(D_{11}+D_{12}-2D_{13}+D_{23}+D_{24}-D_{25}-D_{26}))\times[p_2,-p_4,-p_3,m_i,m_t,m_t,m_t]-2D_{27}[-p_2,p_4,p_3,m_t,m_i,m_i,m_i]-2Q_tD_{27}[-p_1+p_3,p_1,-p_1+p_4,m_i,m_t,m_i,m_t]\}],$$

$$f_2^{b(\hat{t})}=2\sum_{i=H^+,G^+}[g_i^+m_b\{D_{311}[-p_2,p_4,p_3,m_t,m_i,m_i,m_i]-Q_t^2(D_{27}+D_{311})[p_2,-p_4,-p_3,m_i,m_t,m_t,m_t]+Q_t(D_{312}-D_{27}-D_{311}-D_{313})[-p_1+p_3,p_1,-p_1+p_4,m_i,m_t,m_i,m_t]\}-g_i^-m_t\{D_{27}[-p_2,p_4,p_3,m_t,m_i,m_i,m_i]+Q_t^2D_{27}[p_2,-p_4,-p_3,m_i,m_t,m_t,m_t]+Q_tD_{27}[-p_1+p_3,p_1,-p_1+p_4,m_i,m_t,m_i,m_t]\}],$$

$$f_3^{b(\hat{t})}=2\sum_{i=H^+,G^+}g_i^+\{Q_t^2(6D_{313}-2D_{27}-4D_{311}+m_b^2(D_{11}-D_{13}+2D_{21}+2D_{23}-4D_{25}+D_{31}-2D_{33}-3D_{35}+4D_{37})-m_t^2(D_{11}-D_{12})+2(p_1\cdot p_2)(D_{23}-D_{25}-D_{33}-D_{35}+2D_{37})-2(p_1\cdot p_4)(D_{23}-D_{25}-D_{310}-D_{33}+D_{37}+D_{39})-2(p_2\cdot p_4)(2D_{23}+D_{24}-2D_{25}-D_{26}-2D_{310}-D_{33}+D_{34}-D_{35}+2D_{37}+D_{39}))[p_2,-p_4,-p_3,m_i,m_t,m_t,m_t]+Q_t(4D_{312}-2D_{27}-4D_{311}+m_b^2(D_{11}-D_{12}+2D_{21}-2D_{24}+D_{31}+2D_{38}-2D_{310}-D_{32}-D_{34}+D_{36}+D_{37}-D_{39})+m_t^2(D_{12}-D_{11})+2(p_1\cdot p_2)(D_{24}-D_{22}-D_{25}+D_{26}+D_{310}+D_{34}-D_{35}-D_{36})+2(p_1\cdot p_4)(D_{22}-D_{24}+D_{25}-D_{26}-D_{34}+D_{35}+D_{36}-D_{37}-D_{38}+D_{39})+2(p_2\cdot p_4)(D_{24}-D_{21}+D_{25}-D_{26}-D_{31}-D_{310}+D_{34}+D_{35}))\times[-p_1+p_3,p_1,-p_1+p_4,m_i,m_t,m_i,m_t]-2(D_{27}+D_{312})[-p_2,p_4,p_3,m_t,m_i,m_i,m_i]\},$$

$$f_4^{b(\hat{t})}=2\sum_{i=H^+,G^+}\{g_i^+\{Q_t^2(m_b^2(2D_{33}-D_{13}+D_{35}-2D_{37})-4D_{313}-m_t^2D_{13}+2(p_1\cdot p_2)(D_{33}-D_{37})-2(p_1\cdot p_4)(D_{33}-D_{39})+2(p_2\cdot p_4)(D_{23}-D_{25}-D_{310}-D_{33}+D_{37}+D_{39}))[p_2,-p_4,-p_3,m_i,m_t,m_t,m_t]-2D_{313}[-p_2,p_4,p_3,m_t,m_i,m_i,m_i]+2Q_t(D_{313}-D_{312})[-p_1+p_3,p_1,-p_1+p_4,m_i,m_t,m_i,m_t]\}-g_i^-Q_t^22m_bm_tD_{13}[p_2,-p_4,-p_3,m_i,m_t,m_t,m_t]\},$$

$$f_5^{b(\hat{t})}=4\sum_{i=H^+,G^+}g_i^+\left\{(D_{311}-D_{312})[-p_2,p_4,p_3,m_t,m_i,m_i,m_i]+\frac{1}{2}Q_t(4D_{313}+m_b^2(2D_{39}-D_{13}-2D_{25}-D_{33}-D_{35}-D_{38})+m_t^2D_{13}+2(p_1\cdot p_2)(D_{23}-D_{26}-D_{310}+D_{37})+2(p_1\cdot p_4)(D_{310}-D_{23}+D_{26}+D_{33}-D_{37}-D_{39})+2(p_2\cdot p_4)(D_{25}-D_{23}+D_{35}-D_{37}))[-p_1+p_3,p_1,-p_1+p_4,m_i,m_t,m_i,m_t]\right\},$$

$$f_6^{b(\hat{t})}=2\sum_{i=H^+,G^+}\{g_i^+\{Q_t^2(2(D_{313}-D_{311})+m_b^2(D_0+2D_{11}-2D_{13}+D_{21}-2D_{25})+m_t^2D_0+2(p_1\cdot p_4)(D_{25}-D_{26}))\times[p_2,-p_4,-p_3,m_i,m_t,m_t,m_t]+2(D_{27}+D_{311}-D_{313})[-p_2,p_4,p_3,m_t,m_i,m_i,m_i]-2Q_t(D_{27}+D_{311})\times[-p_1+p_3,p_1,-p_1+p_4,m_i,m_t,m_i,m_t]\}+g_i^-Q_t^22m_bm_t(D_0+D_{11}-D_{13})[p_2,-p_4,-p_3,m_i,m_t,m_t,m_t]\},$$

$$f_7^{b(\hat{t})}=4\sum_{i=H^+,G^+}[g_i^+m_b\{Q_t^2(D_{26}+D_{310})[p_2,-p_4,-p_3,m_i,m_t,m_t,m_t]+Q_t(D_{22}-D_{24}+D_{25}-D_{26}-D_{32}-D_{34}+D_{35}+2D_{36}$$
$$+D_{37}+2D_{38}-D_{39}-3D_{310})[-p_1+p_3,p_1,-p_1+p_4,m_i,m_t,m_i,m_t]-(D_{25}+D_{310})[-p_2,p_4,p_3,m_t,m_i,m_i,m_i]\}$$
$$+g_i^-m_t\{Q_t^2D_{26}[p_2,-p_4,-p_3,m_i,m_t,m_t,m_t]+(D_{13}+D_{26})[-p_2,p_4,p_3,m_t,m_i,m_i,m_i]$$
$$+Q_t(D_{22}-D_{24}+D_{25}-D_{26})[-p_1+p_3,p_1,-p_1+p_4,m_i,m_t,m_i,m_t]\}],$$

$$f_8^{b(\hat{t})}=4\sum_{i=H^+,G^+}[g_i^+m_b\{Q_t^2(D_{26}+D_{310}-D_{25}-D_{35})[p_2,-p_4,-p_3,m_i,m_t,m_t,m_t]+Q_t(D_{26}-D_{23}-D_{33}-D_{37}-D_{38}+2D_{39}$$
$$+D_{310})[-p_1+p_3,p_1,-p_1+p_4,m_i,m_t,m_i,m_t]+(D_{35}-D_{310})[-p_2,p_4,p_3,m_t,m_i,m_i,m_i]\}$$
$$+g_i^-m_t\{Q_t^2(D_{26}-D_{25})[p_2,-p_4,-p_3,m_i,m_t,m_t,m_t]+(D_{26}-D_{25})[-p_2,p_4,p_3,m_t,m_i,m_i,m_i]$$
$$+Q_t(D_{26}-D_{23})[-p_1+p_3,p_1,-p_1+p_4,m_i,m_t,m_i,m_t]\}],$$

$$f_9^{b(\hat{t})}=4\sum_{i=H^+,G^+}[g_i^+m_b\{Q_t^2(D_{310}-D_{12}-2D_{24}+D_{26}-D_{34})[p_2,-p_4,-p_3,m_i,m_t,m_t,m_t]+Q_t(D_{12}-D_{11}-2D_{21}-D_{22}$$
$$+3D_{24}-D_{25}+D_{26}-D_{31}+2D_{34}-D_{35}-D_{36}+D_{310})[-p_1+p_3,p_1,-p_1+p_4,m_i,m_t,m_i,m_t]+(D_{11}+D_{21}+D_{24}-D_{25}$$
$$-D_{310}+D_{34})[-p_2,p_4,p_3,m_t,m_i,m_i,m_i]\}+g_i^-m_t\{Q_t^2(D_{26}-D_{12}-D_{24})[p_2,-p_4,-p_3,m_i,m_t,m_t,m_t]$$
$$+(D_{13}-D_0-D_{11}-D_{12}-D_{24}+D_{26})[-p_2,p_4,p_3,m_t,m_i,m_i,m_i]+Q_t(D_{12}-D_{11}-D_{21}+D_{24})$$
$$\times[-p_1+p_3,p_1,-p_1+p_4,m_i,m_t,m_i,m_t]\}],$$

$$f_{10}^{b(\hat{t})}=4\sum_{i=H^+,G^+}[g_i^+m_b\{Q_t^2(D_{11}+2D_{21}-D_{25}+D_{31}-D_{35}-D_{12}-2D_{24}+D_{26}+D_{310}-D_{34})[p_2,-p_4,-p_3,m_i,m_t,m_t,m_t]$$
$$+Q_t(D_{13}+D_{23}+2D_{25}-D_{26}+D_{35}+D_{37}-D_{310})[-p_1+p_3,p_1,-p_1+p_4,m_i,m_t,m_i,m_t]+(D_{24}-D_{21}-D_{31}+D_{34}$$
$$+D_{35}-D_{310})[-p_2,p_4,p_3,m_t,m_i,m_i,m_i]\}+g_i^-m_t\{Q_t^2(D_{11}+D_{21}-D_{25}-D_{12}-D_{24}+D_{26})$$
$$\times[p_2,-p_4,-p_3,m_i,m_t,m_t,m_t]+(D_{11}-D_{12}+D_{21}-D_{24}-D_{25}+D_{26})[-p_2,p_4,p_3,m_t,m_i,m_i,m_i]+Q_t(D_{32}+D_{25})$$
$$\times[-p_1+p_3,p_1,-p_1+p_4,m_i,m_t,m_i,m_t]\}],$$

$$f_{11}^{b(\hat{t})}=\sum_{i=H^+,G^+}[g_i^+\{Q_t^2(4(D_{313}-D_{312})+m_b^2(D_0+D_{12}-D_{13}-D_{21}+2D_{24}-2D_{26}-2D_{310}-2D_{33}+D_{34}-D_{35}+2D_{37}+2D_{39})$$
$$+m_t^2(D_0-D_{12}+D_{13})+2(p_1\cdot p_2)(D_{25}-D_{26}-D_{310}-D_{33}+D_{37}+D_{39})+2(p_1\cdot p_4)(D_{33}+D_{38}-2D_{39})+2(p_2\cdot p_4)(D_{33}$$
$$-D_{22}-D_{23}+2D_{26}+2D_{310}-D_{36}-D_{37}+D_{38}-2D_{39}))[p_2,-p_4,-p_3,m_i,m_t,m_t,m_t]$$
$$+2(D_{313}-D_{312})[-p_2,p_4,p_3,m_t,m_i,m_i,m_i]+2Q_t(D_{311}-D_{313})[-p_1+p_3,p_1,-p_1+p_4,m_i,m_t,m_i,m_t]\}$$
$$+g_i^-Q_t^22m_bm_tD_0[p_2,-p_4,-p_3,m_i,m_t,m_t,m_t]],$$

$$f_{12}^{b(\hat{t})}=2\sum_{i=H^+,G^+}g_i^+\{Q_t^2(D_{27}+D_{312}-D_{313})[p_2,-p_4,-p_3,m_i,m_t,m_t,m_t]+(D_{313}-D_{312})[-p_2,p_4,p_3,m_t,m_i,m_i,m_i]$$
$$+Q_t(D_{27}+D_{311}-D_{313})[-p_1+p_3,p_1,-p_1+p_4,m_i,m_t,m_i,m_t]\},$$

$$f_{13}^{b(\hat{t})}=2Q_t\sum_{i=H^+,G^+}[g_i^+m_b\{(D_{12}-D_{11}-D_{21}-D_{22}+2D_{24}-D_{25}+D_{26})[-p_1+p_3,p_1,-p_1+p_4,m_i,m_t,m_i,m_t]-Q_t(D_{12}$$
$$+D_{24})[p_2,-p_4,-p_3,m_i,m_t,m_t,m_t]\}+g_i^-m_t\{(D_{12}-D_{11})[-p_1+p_3,p_1,-p_1+p_4,m_i,m_t,m_i,m_t]$$
$$-Q_tD_{12}[p_2,-p_4,-p_3,m_i,m_t,m_t,m_t]\}],$$

$$f_{14}^{b(\hat{t})}=2Q_t^2\sum_{i=H^+,G^+}\{g_i^+m_b(D_{13}+D_{25})[p_2,-p_4,-p_3,m_i,m_t,m_t,m_t]+g_i^-m_tD_{13}[p_2,-p_4,-p_3,m_i,m_t,m_t,m_t]\},$$

$$f_{15}^{b(\hat{t})}=2Q_t\sum_{i=H^+,G^+}[g_i^+m_b\{Q_t(D_{11}-D_{12}+D_{21}-D_{24})[p_2,-p_4,-p_3,m_i,m_t,m_t,m_t]+(D_{13}+D_{23}+D_{25}-D_{26})$$
$$\times[-p_1+p_3,p_1,-p_1+p_4,m_i,m_t,m_i,m_t]\}+g_i^-m_t\{Q_t(D_{11}-D_{12})[p_2,-p_4,-p_3,m_i,m_t,m_t,m_t]$$
$$+D_{13}[-p_1+p_3,p_1,-p_1+p_4,m_i,m_t,m_i,m_t]\}],$$

$$f_{16}^{b(\hat{t})}=2Q_t^2\sum_{i=H^+,G^+}\{g_i^+m_b(D_{13}-D_{11}+D_{25}-D_{21})[p_2,-p_4,-p_3,m_i,m_t,m_t,m_t]+g_i^-m_t(D_{13}-D_{11})$$
$$\times[p_2,-p_4,-p_3,m_i,m_t,m_t,m_t]\},$$

$$f_{17}^{b(\hat{t})}=4\sum_{i=H^+,G^+}g_i^+\{Q_t^2(D_{23}-D_{26}-D_{38}+D_{39})[p_2,-p_4,-p_3,m_i,m_t,m_t,m_t]+(D_{26}-D_{23}+D_{38}-D_{39})$$
$$\times[-p_2,p_4,p_3,m_t,m_i,m_i,m_i]+Q_t(D_{24}-D_{22}-D_{25}+D_{26}+D_{34}-D_{35}-D_{36}+D_{37}+D_{38}-D_{39})$$
$$\times[-p_1+p_3,p_1,-p_1+p_4,m_i,m_t,m_i,m_t]\},$$

$$f_{18}^{b(\hat{t})}=4\sum_{i=H^+,G^+}g_i^+\{Q_t^2(D_{25}-D_{26}+D_{310}-D_{37}+D_{39}-D_{38})[p_2,-p_4,-p_3,m_i,m_t,m_t,m_t]$$
$$+(D_{37}+D_{38}-D_{39}-D_{310})[-p_2,p_4,p_3,m_t,m_i,m_i,m_i]+Q_t(D_{23}-D_{26}-D_{33}+D_{37}+D_{39}-D_{310})$$
$$\times[-p_1+p_3,p_1,-p_1+p_4,m_i,m_t,m_i,m_i]\},$$

$$f_{19}^{b(\hat{t})}=4\sum_{i=H^+,G^+}g_i^+\{Q_t^2(D_{22}+D_{23}-D_{25}-D_{26}+D_{36}-D_{38}+D_{39}-D_{310})[p_2,-p_4,-p_3,m_i,m_t,m_t,m_t]+(D_{13}-D_{12}-D_{22}$$
$$-D_{23}-D_{24}+D_{25}+2D_{26}-D_{36}+D_{38}-D_{39}+D_{310})[-p_2,p_4,p_3,m_t,m_i,m_i,m_i]+Q_t(D_{21}-D_{24}-D_{25}+D_{26}+D_{31}-D_{34}$$
$$-D_{35}+D_{310})[-p_1+p_3,p_1,-p_1+p_4,m_i,m_t,m_i,m_t]\},$$

$$f_{20}^{b(\hat{t})}=4\sum_{i=H^+,G^+}g_i^+\{Q_t^2(D_{22}-D_{24}+D_{25}-D_{26}-D_{34}+D_{35}+D_{36}-D_{37}+D_{39}-D_{38})[p_2,-p_4,-p_3,m_i,m_t,m_t,m_t]+(D_{24}$$
$$-D_{22}-D_{25}+D_{26}+D_{34}-D_{35}-D_{36}+D_{37}+D_{38}-D_{39})[-p_2,p_4,p_3,m_t,m_i,m_i,m_i]+Q_t(D_{23}-D_{25}-D_{35}+D_{37})$$
$$\times[-p_1+p_3,p_1,-p_1+p_4,m_i,m_t,m_i,m_t]\},$$

$$f_1^{\rm tr}=\sum_{i=H^+,G^+}\{g_i^+m_bC_{11}-g_i^-m_tC_0\}[-p_2,p_1+p_2,m_t,m_i,m_i],$$

where

$$(p_3-p_1)^2=\hat{t},\quad \hat{s}=(p_1+p_2)^2,$$

$$2p_1\cdot p_3=2p_2\cdot p_4=m_b^2-\hat{t},$$

$$2p_3\cdot p_4=\hat{s},\quad 2p_1\cdot p_4=2p_2\cdot p_3=m_b^2-\hat{u},$$

$$2p_1\cdot p_2=\hat{s}-2m_b^2,\quad \hat{s}+\hat{t}+\hat{u}=2m_b^2,$$

$$\eta_i=\begin{cases}\cot^2\beta, & i=H^\pm,\\ 1, & i=G^\pm.\end{cases}$$

APPENDIX B

The cross section of the subprocess $\gamma\gamma\to b\bar{b}$ can be calculated from Eqs. (1)–(15). Then we summarize the interference term with explicit form as

$$2\sum_{\text{spins}}\overline{M_0^{\dagger}\cdot \delta M_1}_{\text{ loop}}=\frac{-e^4Q_b^2}{2\sqrt{\hat{s}}}\left\{\frac{A_1}{\sqrt{\hat{s}}+\sqrt{\hat{s}-4m_b^2}\cos\theta}+\frac{A_2}{\sqrt{\hat{s}}-\sqrt{\hat{s}-4m_b^2}\cos\theta}\right\},$$

where θ is the angle between the outgoing bottom quark and one of the incoming photons in the center-of-mass system and A_1 and A_2 in the above equation are defined as

$$A_1=-32m_b^3(F_1+F_2)+32m_b^4(F_2+F_4-F_5-F_6)+32m_b^5(F_8+F_9-F_7-F_{10})+16m_b\hat{s}(2F_1-F_2)+24m_b^2\hat{s}(F_{11}-F_{12})$$
$$+4m_b^2\hat{s}(F_4-F_3-F_5+F_6)+8m_b^2\hat{s}(2F_{10}+3F_{14}-3F_{16}+2F_7-F_8-3F_9)+4\hat{s}^2(F_6-F_3-F_{12})+2m_b\hat{s}^2(2F_9-F_{10}$$
$$-F_{13}-F_{14}-F_{15}-F_7+5F_{16})+m_b^2\hat{s}^2(3F_{19}-F_{17}-F_{18}-F_{20})-\hat{s}^3F_{19}+\sqrt{\hat{s}(\hat{s}-4m_b^2)}\cos\theta[16m_b(F_1-2F_2)$$
$$+4m_b^2(F_5+F_6-F_3-F_4+2F_{11}+2F_{12})+4m_b^3(F_7-F_8-F_9+F_{10}-2F_{13}-2F_{14}+2F_{15}+2F_{16})+8m_b^4(F_{17}-F_{18}$$
$$-F_{19}+F_{20})+4\hat{s}(F_6-F_3)-2m_b\hat{s}(F_7+F_{10}+2F_{13})+2m_b^2\hat{s}(2F_{19}-F_{17}-F_{20})]+\hat{s}\cos^2\theta[-16m_b^2F_{12}+8m_b^3(F_{13}$$
$$-F_{14}-F_{15}+F_{16})+4m_b^4(F_{17}-F_{18}-F_{19}+F_{20})+4\hat{s}F_{12}+2m_b\hat{s}(F_{14}-F_{13}+F_{15}-F_{16})+m_b^2\hat{s}(F_{18}-F_{17}-3F_{19}-F_{20})$$
$$+\hat{s}^2F_{19}],$$

$$A^2=-32m_b^3(F_1+F_2)+32m_b^4(F_3+F_4-F_5-F_6)+32m_b^5(F_8-F_7+F_9-F_{10})+16m_b\hat{s}(2F_2-F_1)+4m_b^2\hat{s}(F_3-F_4+F_5$$
$$-F_6+2F_{11}-2F_{12})+8m_b^3\hat{s}(2F_7-3F_8-F_9+2F_{10}+2F_{13}+3F_{14}-2F_{15}-3F_{16})+4\hat{s}^2(F_5-F_4+2F_{12}-F_{11})$$
$$+2m_b\hat{s}^2(2F_8-F_7-F_{10}-F_{13}-5F_{14}+2F_{15}+F_{16})+m_b^2\hat{s}^2(F_{17}-3F_{18}+F_{19}+F_{20})+\hat{s}^2F_{18}$$
$$+\sqrt{\hat{s}(\hat{s}-4m_b^2)}\cos\theta[16m_b(2F_1-F_2)+4m_b^2(F_3+F_4-F_5-F_6+2F_{11}+2F_{12})+4m_b^3(F_8-F_7+F_9-F_{10}-2F_{13}$$
$$-2F_{14}+2F_{15}+2F_{16})+8m_b^4(F_{17}-F_{18}-F_{19}+F_{20})+4\hat{s}(F_4-F_5+2F_{11}-2F_{12})+2m_b\hat{s}(F_7+F_{10}+2F_{13}+4F_{14}$$
$$-4F_{15})+2m_b^2\hat{s}(2F_{18}-F_{17}-F_{20})]+\hat{s}\cos^2\theta[16m_b^2F_{11}+8m_b^3(F_{13}-F_{14}-F_{15}+F_{16})+4m_b^4(F_{18}-F_{17}+F_{19}-F_{20})$$
$$-4\hat{s}F_{11}+2m_b\hat{s}(F_{14}-F_{13}+F_{15}-F_{16})+m_b^2\hat{s}(F_{17}+3F_{18}-F_{19}+F_{20})-\hat{s}^2F_{18}],$$

where the Lorentz invariant factors F_i used above are defined to be expressed by the form factors which are shown in Eq. (6)–(14). Their explicit expressions are listed below:

$$F_1=\sum_{j=\hat{t},\hat{u}}\left[\frac{-Q_b^2}{(\hat{t}-m_b^2)^2}f_1^{s(j)}+\frac{Q_b}{\hat{t}-m_b^2}f_1^{v(j)}+\frac{1}{16\pi^2}f_1^{b(j)}\right]-\frac{1}{16\pi^2}f_1^{\text{tr}},$$

$$F_2=\sum_{j=\hat{t},\hat{u}}\frac{1}{16\pi^2}f_2^{b(j)}-\frac{1}{16\pi^2}f_1^{\text{tr}},$$

$$F_3=\sum_{j=\hat{t},\hat{u}}\left[\frac{Q_b}{\hat{t}-m_b^2}f_2^{v(j)}+\frac{1}{16\pi^2}f_3^{b(j)}\right],$$

$$F_4=\sum_{j=\hat{t},\hat{u}}\frac{1}{16\pi^2}f_4^{b(j)},$$

$$F_5=\sum_{j=\hat{t},\hat{u}}\frac{1}{16\pi^2}f_5^{b(j)},$$

$$F_6=\sum_{j=\hat{t},\hat{u}}\left[\frac{-Q_b^2}{(\hat{t}-m_b^2)^2}f_2^{s(j)}+\frac{Q_b}{\hat{t}-m_b^2}f_3^{v(j)}+\frac{1}{16\pi^2}f_6^{b(j)}\right],$$

$$F_7=\sum_{j=\hat{t},\hat{u}}\frac{1}{16\pi^2}f_7^{b(j)},$$

$$F_8=\sum_{j=\hat{t},\hat{u}}\frac{1}{16\pi^2}f_8^{b(j)},$$

$$F_9=\sum_{j=\hat{t},\hat{u}}\left[\frac{Q_b}{\hat{t}-m_b^2}f_4^{v(j)}+\frac{1}{16\pi^2}f_9^{b(j)}\right],$$

$$F_{10}=\sum_{j=\hat{t},\hat{u}}\frac{1}{16\pi^2}f_{10}^{b(j)},$$

$$F_{11}=\sum_{j=\hat{t},\hat{u}}\left[\frac{-Q_b^2}{(\hat{t}-m_b^2)^2}f_3^{s(j)}+\frac{Q_b}{\hat{t}-m_b^2}f_5^{v(j)}+\frac{1}{16\pi^2}f_{11}^{b(j)}\right],$$

$$F_{12}=\sum_{j=\hat{t},\hat{u}}\frac{1}{16\pi^2}f_{12}^{b(j)},$$

$$F_{13}=\sum_{j=\hat{t},\hat{u}}\left[\frac{Q_b}{\hat{t}-m_b^2}f_6^{v(j)}+\frac{1}{16\pi^2}f_{13}^{b(j)}\right],$$

$$F_{14}=\sum_{j=\hat{t},\hat{u}}\frac{1}{16\pi^2}f_{14}^{b(j)},$$

$$F_{15}=\sum_{j=\hat{t},\hat{u}} \frac{1}{16\pi^2} f_{15}^{b(j)},$$

$$F_{16}=\sum_{j=\hat{t},\hat{u}} \left[\frac{Q_b}{\hat{t}-m_b^2} f_7^{v(j)} + \frac{1}{16\pi^2} f_{16}^{b(j)} \right],$$

$$F_{17}=\sum_{j=\hat{t},\hat{u}} \frac{1}{16\pi^2} f_{17}^{b(j)},$$

$$F_{18}=\sum_{j=\hat{t},\hat{u}} \frac{1}{16\pi^2} f_{18}^{b(j)},$$

$$F_{19}=\sum_{j=\hat{t},\hat{u}} \frac{1}{16\pi^2} f_{19}^{b(j)},$$

$$F_{20}=\sum_{j=\hat{t},\hat{u}} \frac{1}{16\pi^2} f_{20}^{b(j)}.$$

[1] Stanley J. Brodsky and Peter M. Zerwas, Nucl. Instrum. Methods A **355**, 19 (1995).

[2] I. F. Ginzburg, G. L. Kotkin, V. G. Serbo, and V. I. Telnov, Zh. Eksp. Teor. Fiz. **34**, 514 (1981); Nucl. Instrum. Methods. **205**, 47 (1983).

[3] R. J. Nobel, Nucl. Instrum. Methods A **256**, 427 (1987); R. Blankenbecler and S. D. Drell, Phys. Rev. D **36**, 277 (1987); **37**, 3308 (1988); Phys. Rev. Lett. **61**, 2324 (1988); R. Blankenbecler, S. D. Drell, and N. Kroll, Phys. Rev. D **40**, 2462 (1989); M. Jacob and T. T. Wu, Phys. Lett. B **197**, 253 (1987); Nucl. Phys. **B303**, 373 (1988); **B303**, 389 (1988); **B314**, 334 (1989); **B318**, 53 (1989).

[4] R. Blankenbecler and S. D. Drell, Phys. Rev. Lett. **61**, 2324 (1988); D. V. Schroeder, SLAC Report No. 371, 1990 (unpublished).

[5] V. Telnov, Nucl. Instrum. Methods A **294**, 72 (1990); I. Ginzburg, G. Kotkin, V. Serbo, and V. Telnov, *ibid.* **205**, 47 (1984); **219**, 5 (1984).

[6] F. Halzen, C. S. Kim, and M. L. Stong, Phys. Lett. B **274**, 489 (1992); P. Zerwas, in *Physics and Experiments with Linear Colliders*, Proceedings of the Workshop, Saariselkä, Finland, 1991, edited by R. Orava, P. Eerola, and M. Nordberg (World Scientific, Singapore, 1992).

[7] O. J. P. Eboli, M. C. Gonzalez-Garcia, F. Halzen, and S. F. Novaes, Phys. Rev. D **47**, 1889 (1993).

[8] A. Denner, Fortschr. Phys. **41**, 307 (1993).

[9] For a view, see, for example, J. F. Gunion, H. E. Haber, G. Kane, and S. Dawson, *The Higgs Hunter's Guide* (Addison-Wesley, Reading, MA, 1990).

[10] A. Sirlin, Phys. Rev. D **22**, 971 (1980); W. J. Marciano and A. Sirlin, *ibid.* **22**, 2695 (1980); **31**, 213(E) (1985); A. Sirlin and W. J. Marciano, Nucl. Phys. **B189**, 442 (1981); M. Bohm, W. Hollik, and H. Spiesberger, Fortschr. Phys. **34**, 687 (1986).

[11] W. Hollik, Z. Phys. C **32**, 291 (1986); **37**, 569 (1988); W. J. Marciano and Z. Parsa, Annu. Rev. Nucl. Sci. **36**, 171 (1986).

[12] M. Drees and R. M. Godbole, Phys. Rev. Lett. **67**, 1189 (1991).

[13] Particle Data Group, L. Montanet *et al.*, Phys. Rev. D **50**, 1173 (1994); D. Schaile, in *Proceedings of the 27th International Conference on High Energy Physics*, Glasgow, Scotland, 1990, edited by P. J. Bussey and I. G. Knowles (IOP, London, 1995).